Tome 39 N° 12 DÉCEMBRE 1978

LE JOURNAL DE PHYSIQUE

Classification
Physics Abstracts
44.25 — 47.25Q

NON BOUSSINESQ CONVECTIVE STRUCTURES IN WATER NEAR 4 °C

M. DUBOIS, P. BERGE and J. WESFREID

DPh-G/PSRM, CEN Saclay, B.P. n° 2, 91190 Gif sur Yvette, France

(*Reçu le 7 juillet 1978, accepté le 29 août 1978*)

Résumé. — Des mesures de vitesse locale effectuées dans une couche d'eau en convection au voisinage de 4 °C sont présentées. La répartition non linéaire de la densité de l'eau produit des effets convectifs qualitativement différents de ceux que l'on observe dans le cas des fluides répondant à l'approximation de Boussinesq. On trouve en particulier des structures convectives hexagonales près du seuil critique, structures qui apparaissent par une bifurcation anormale. Ces hexagones se transforment à plus haut nombre de Rayleigh en rouleaux dissymétriques, cette transformation étant réversible mais s'accompagnant d'une hystérésis importante. L'ensemble des comportements observés est cohérent avec la brisure de symétrie des propriétés de la couche.

Abstract. — The convective properties of a water layer near 4 °C have been examined by means of local velocity measurements. The non linear density profile of such a layer produces qualitatively different behaviour from that observed in « Boussinesq » fluids. In particular a hexagonal dissipative structure is observed corresponding to an abnormal bifurcation near the threshold ; at higher Rayleigh numbers, these hexagons transform into asymmetric two-dimensional rolls. The measured velocity field is in agreement with that expected from the breakdown in the symmetry properties of the water layer.

1. **Introduction.** — It is well known that the preferred dissipative structure for a « Boussinesq » fluid near its Rayleigh-Bénard instability threshold consists of two-dimensional rolls (see for example the references in [1] and [2]). Let us recall that the Rayleigh-Bénard instability is related to the buoyancy driven motion in a layer of a pure fluid confined between two horizontal conducting rigid plates ; the horizontal extension of this layer is supposed to be much greater than its depth d. Under such conditions, if the temperature difference ΔT across the layer is higher than a critical value (the lower plate being at the higher temperature), ordered convective motion takes place in the layer. More precisely, the properties of this layer are described by the Rayleigh number

$$R = \frac{g\alpha\,\Delta T d^3}{\nu D_T} \qquad (1)$$

where g is the gravitational acceleration, and α, ν and D_T are respectively the volume expansion coefficient, the kinematic viscosity and the thermal diffusivity of the fluid. The critical threshold of instability is $R_c = 1\,707$ in infinite geometry. The Boussinesq assumption consists in neglecting the temperature variation of the physical properties of the fluid, except for that of the density. Under such conditions, the properties of the unstable layer are symmetric with respect to the mid-plane of the layer : local velocity measurements [2] as well as temperature measurements [3], [4] show a perfect symmetry between the downward and upward motion. Then, in the mid-plane of the cell, the vertical velocity component V_Z obeys the relation (near the threshold)

$$V_Z = \tilde{V}_Z \cos \frac{2\pi X}{\Lambda_c}$$

where X is the coordinate along the greatest extension of the cell, perpendicular to the axis of the rolls and Λ_c is the wavelength of the preferred mode. Near the threshold $\Lambda_c \sim 2\,d$.

The equiprobability of having either $+V$ or $-V$ at any point in the fluid is characteristic of a normal bifurcation. The main consequence of such a behaviour is a striking similarity between some properties of the Rayleigh-Bénard instability and those of second order phase transitions [5].

Non Boussinesq case. — If the physical properties of the convective fluid vary strongly with temperature, or more generally, if they are different at the bottom and at the top boundaries, we may expect an asymmetry between the upward and downward motion. The first example of such a flow is given by the hexagonal pattern of Bénard's experiments [6]. In the case of rigid-rigid horizontal boundaries, such an hexagonal pattern has been predicted in [7] and [8] in relation with the variation of the physical properties of the fluid in the layer and has been observed in fluids with high viscosity variations [9], [10], [11].

If we consider the properties of water near 4 °C, where the coefficient of volume expansion varies from zero to finite values, we also expect to have an asymmetric dissipative structure. The aim of the work reported here is to study this convective structure in a layer of water, where the isotherm 4 °C is applied to the top boundary, the bottom plate being at a higher temperature. In this geometry, the buoyancy forces which are driving the instability are greater at the bottom plate and we may expect to have upward motion with a greater amplitude than that of the downward flow leading to an asymmetric dissipative structure (div $\rho V = 0$).

2. **Experimental arrangement.** — The cell, which contains the water, has already been described [12]. It is rectangular with horizontal extension $18 \times 7.5\ \text{cm}^2$ and is 1 cm high. The top and bottom plates which confine horizontally the water layer are thermally regulated by circulating water from cooled thermostatic baths. The over-all thermal precision is $\pm\ 5 \times 10^{-2}$ °C. The water is confined laterally by a plexiglass rectangular frame through which all optical measurements are made. In all the results reported in this paper, the top plate temperature is kept at 4.15 °C.

The convective structure was studied by local velocity measurements, in particular the vertical velocity component V_Z. This component was measured in the mid-height-plane of the layer by a laser-Doppler anemometer which works according to the real fringe mode. The signal from the photomultiplier is processed by a real time Fourier analyser. The measurement volume is approximately :

$$\delta X \times \delta Z \times \delta Y = 0.15 \times 0.15 \times 1.3\ \text{mm}^3 .$$

$Z'Z$ is the vertical axis ; $X'X$ and $Y'Y$ are the horizontal ones, respectively parallel to the greatest and the shortest side of the cell.

3. **Experimental results.** — 3.1 CONVECTION THRESHOLD. — The threshold of the convective motion is evidenced by the appearance of measurable velocities in the water layer. The top plate being at 4.15 °C, the corresponding ΔT_c is 1.94 ± 0.05 °C. If we calculate the corresponding Rayleigh number as

$$R = \frac{gd^3}{vD_T}\left(\frac{\Delta\rho}{\rho_0}\right) \qquad (2)$$

where $\Delta\rho$ is the density difference between the bottom and top plates, we obtain $R_c = 1\,660 \pm 120$. The relation giving the variation of ρ with the temperature T is, near 4 °C :

$$\rho \simeq \rho_0[1 - \beta(T - T_{max})^2] .$$

with $\beta = 8.1 \times 10^{-6}$ and $T_{max} = 3.98$ °C.

At $T = 5$ °C

$$D_T = 1.37 \times 10^{-3}\ \text{cm}^2\ \text{s}^{-1}$$

and

$$v = 1.519 \times 10^{-2}\ \text{cm}^2\ \text{s}^{-1} \quad (P = 11.1) .$$

In the limit of our experimental accuracy, we see that the critical Rayleigh number is nearly the same as in the Boussinesq case. Moreover this result is in agreement with the calculated and experimentally observed value given in [13], and is of the same order of magnitude as that mentioned in [14]. We must note also that we do not observe — within the limits of the accuracy of our thermal regulation — any hysteresis phenomenon in the value of ΔT_c, that is to say, if this hysteresis exists, it does not exceed a few percent around the observed value.

3.2 CONVECTIVE STRUCTURE. — 3.2.1 *Hexagonal pattern.* — For temperature differences ΔT slightly above ΔT_c, we obtain a structure whose velocity field is represented on figure 1. This picture gives

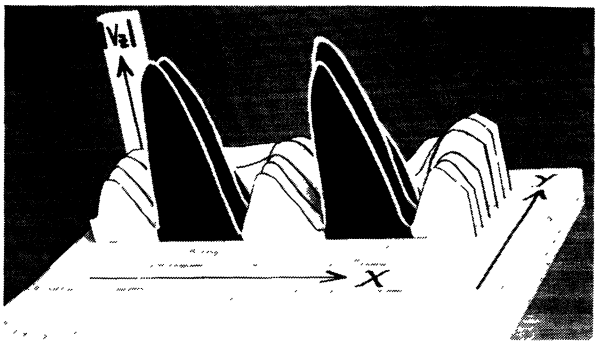

FIG. 1. — Picture of the tridimensional pattern representating the experimental variation of the vertical velocity V_Z (measured at the mid-height of the layer) as a function of the coordinates X and Y in the case of hexagonal structures. The dark areas represent ascending motion.

the spatial variation of the V_Z component, measured in the mid-plane of the cell, where V_Z is maximized *versus* Z. We can see that this tridimensional structure consists of regions with downward velocities which surround smaller regions of higher upward velocities.

Such an arrangement is typical of a hexagonal pattern.

We compared the spatial variation of the V_Z amplitude as measured, with that calculated from the expected dependence for a hexagonal structure [15].

$$V_Z = \frac{1}{3}\tilde{V}_Z\left[4\cos\left[\frac{a}{4}(\sqrt{3}\,x + y)\right] \times \cos\left[\frac{a}{4}(\sqrt{3}\,x - y)\right] \times \cos\frac{a}{2}y - 1\right]$$

$a = 4\,\pi d/3\,L$ is the dimensionless wavenumber of the structure, L is the length of a side of a hexagon, and $\tilde{V}_Z$ is the maximum vertical velocity amplitude located in the centre of a hexagon which is taken here as the origin of the axes. In our experimental geometry the X and Y axes of the hexagonal pattern are found parallel to $X'X$ and $Y'Y$ axes of the cell.

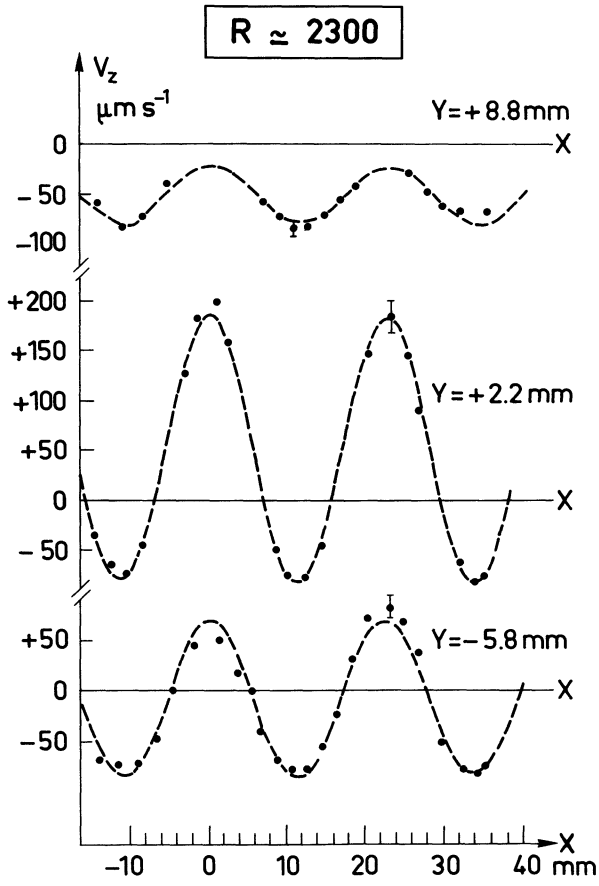

FIG. 2. — $V_Z = f(X)$ characteristics for different Y values in hexagonal structure — the dashed line represents the computer best fit with the theoretical velocity profiles expected for hexagons. The origin $X = 0$, $Y = 0$ is taken at the centre of a hexagon, the X axis is nearly parallel to a line joining the centres of two adjacent hexagons. Positive value of V_Z corresponds to ascending motion.

The results, as shown on figure 2, well demonstrate the presence of a hexagonal structure in the water convective layer, here at $R = 2\,310$. The best fit between measured and calculated values gives

$$\Lambda_x = \sqrt{3}\,L = 22.5 \pm 1 \text{ mm}$$

which corresponds to $a = 3.22 \pm 0.1$ near to the critical value $a_c = 3.117$ [15]. Though all the results are *very* consistent with the presence of hexagons, we have to note that a slight deformation of the pure hexagonal pattern probably occurs due to the influence of boundaries; indeed, the hexagons are only regular in the central part of the cell.

3.2.2 *Asymmetric rolls.* — As ΔT is increased, at a definite value ΔT_1 the hexagonal pattern is transformed into two-dimensional asymmetric rolls, with a wavelength nearly $\Lambda_c = 2\,d$. A typical velocity field of this structure is shown on figure 3, where V_Z is independent of Y. We can note that, as for the case of hexagons, the maximum ascending velocity has always a greater amplitude than the descending velocity.

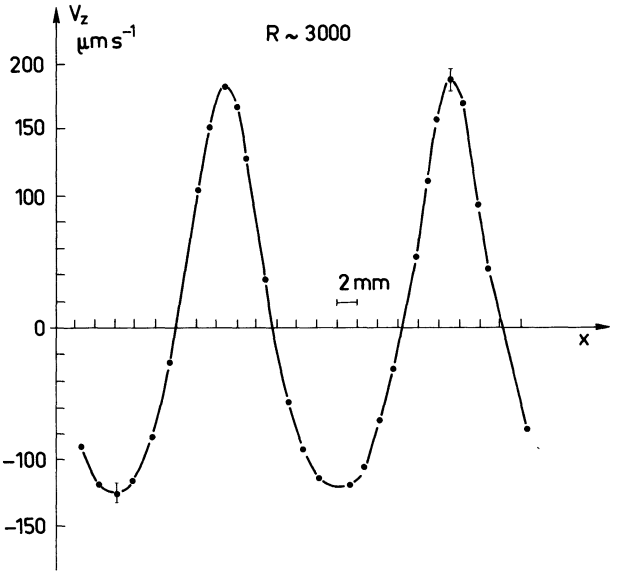

FIG. 3. — Typical characteristic $V_Z = f(X)$ for two dimensional roll structure. The roll axis is along the Y axis, parallel to the short side of the cell.

These two types of structure, hexagons and asymmetric rolls, can be well understood if we consider the actual mechanism of the buoyancy driven convection. As explained before, the stimulation of the motion is greater at the lower horizontal boundary. So our mechanism is similar to that observed by Atten and Lacroix [16] in electrohydrodynamics instabilities, and to that observed by Krishnamurti [17] who observed instabilities in a layer submitted to a non linear temperature gradient. Note furthermore that numerical calculations, performed by Moore and Weiss [18] on two-dimensional structures in water near 4 °C predict the presence of asymmetric ascending and descending flow.

3.3 DEPENDENCE ON R. — We have studied the experimental domain of stability of the hexagonal pattern; then, we measured the variation of the vertical velocity amplitude with R, in the two types

of structure (hexagons and asymmetric rolls). We recall again that in all our measurements, the top plate was maintained at 4.15 °C ± 0.03 °C, and all the structures we studied, correspond to the equilibrium state, ΔT being maintained constant during many hours.

3.3.1 *Hexagonal pattern.* — The hexagonal structure which appears at the threshold of the convective state is stable in a small range of Rayleigh numbers : when we increase ΔT, then R, at $R_2 \simeq 2\,500 \pm 100$ the hexagonal pattern transforms into two-dimensional rolls. Beyond this R_2 value, only the rolls are stable; then, by decreasing ΔT, the hexagonal structure reappears only at $R_1 = 1\,900 \pm 50$ showing, indeed, a notable hysteresis in the transformation rolls ⇆ hexagons.

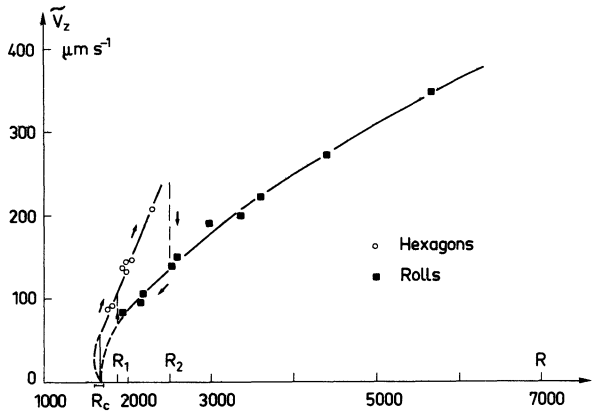

FIG. 4. — Behaviour of the maximum velocity amplitude, $\tilde{V}_Z$, *versus* Rayleigh number for hexagons and rolls.

This phenomenon is illustrated on figure 4 in which we have reported the $\tilde{V}_Z$ maximum amplitude of the ascending flow in the two types of structures.

Considering first the dependence of the velocity amplitude in the hexagonal pattern, two remarks can be made :

a) at R_c, the convective velocity seems to jump discontinuously from zero to a definite value $\tilde{V}_0$ ($\simeq 50\ \mu m\ s^{-1}$);

b) from this value, the amplitude approximately grows as $(R - R_c)$ according to an empirical law

$$\tilde{V}_Z = \left[50 + 450\left(\frac{R - R_c}{R_c}\right)\right] \mu m\ s^{-1}$$

which describes the observed behaviour very near the threshold to within a 10 % accuracy.

3.3.2 *Roll pattern.* — The asymmetric rolls structure has been studied in the range $1\,900 < R < 8\,300$. These rolls are strictly two-dimensional and parallel to Y, that is to say parallel to the short edge of the frame. The asymmetry V_+/V_-, that is the ratio of the maximum amplitude of the ascending and descending motion V_+ and V_- is approximately constant in all of the domain studied, remaining equal to $V_+/V_- = 1.4 \pm 0.1$.

The wavelength Λ, nearly equal to 2 d slightly above the threshold, increases to $\Lambda = 2.35\ d$ at $R_a = 8\,300$. This wavelength variation exhibits hysteresis and time dependence.

From our measurements we have calculated the amplitude $\tilde{V}_Z$ of the fundamental Fourier mode which would give the same mean mass flux as that measured. $\tilde{V}_Z$ varies as

$$\tilde{V}_Z = \tilde{V}_Z^*\left(\frac{R - R_c}{R_c}\right)^{0.49 \pm 0.02}$$

with $\tilde{V}_Z^* = 168\ \mu m\ s^{-1}$, and $R_c \simeq 1\,660$.

Let us note that this power law dependence is the same as that found for Boussinesq conditions, despite the asymmetry of corresponding rolls. Moreover, the value of $\tilde{V}_Z^*$ is in perfect agreement with that calculated in [19] and measured in high Prandtl number fluids [2].

It is also interesting to remark the striking difference of the velocity behaviour with R, for the case of the roll arrangement and for the hexagonal pattern, results which are in agreement with Veronis calculations [21].

4. **Discussion.** — All these results are consistent with the asymmetric properties of a water layer near 4 °C. In particular, in the hexagonal pattern, the non-equivalence of the ascending and descending velocities, leads to a phenomenological Landau equation [19], [5], [20], to which we must add a $\tilde{V}^2$ term such as

$$\tau_0 \frac{d\tilde{V}}{dt} = \tilde{V}\varepsilon + b\tilde{V}^2 - c\tilde{V}^3 \qquad (3)$$

where τ_0 is a characteristic time and $\varepsilon = \dfrac{R - R_c}{R_c}$.

We are in the presence of an abnormal bifurcation. In the stationary state, the solution of this equation is

$$\tilde{V} = \frac{b}{2c} \pm \frac{b}{2c}\left[1 + 4\frac{c}{b^2}\varepsilon\right]^{1/2} \qquad (4)$$

which gives for low values of ε

$$\tilde{V} - \frac{\tilde{V}_0}{2} = \pm \frac{\tilde{V}_0}{2}\left[1 + 2\frac{\tilde{V}_1}{\tilde{V}_0}\varepsilon + \cdots\right] \qquad (5)$$

$\tilde{V}_0$ is the value of the velocity jump at $R = R_c$ and $\tilde{V}_1$ is the extrapolated value at $\varepsilon = 1$ of the velocity behaviour $\tilde{V}_Z - \tilde{V}_0 = f(R)$ measured at low values of ε.

With such a description, we expect to have an hysteresis phenomenon for the threshold R_c, that is to say the established convection is expected to disappear at a value $R' < R_c$ (or at a ε' negative value). The calculation gives $\varepsilon' = -\tilde{V}_0/4\,\tilde{V}_1$, the value

of which equals − 0.028 according to our experimental results (or $R' = 1\,610$). This value is within our experimental accuracy in the R_c determination. Let us note finally that equation (5) predicts that, immediately after the jump, V increases as ε, as observed. The hysteresis of the transformation hexagons ⇆ rolls, has been predicted in [7] and [8] and observed in [9], [10] and [11] in the case of non-Boussinesq conditions. But the comparison with our experiment is not obvious ; for, if we take into account only the variation of the physical constants of the water between the lower and upper plates, the corresponding domain of stability of the hexagonal pattern would be very narrow and not experimentally observable.

So, it would be necessary to perform complete calculations in the specific case of the water volume expansion anomaly. Therefore, our experimental results seem to confirm the fact that the non-linearities are more efficient for the stability of the hexagonal pattern in agreement with the results given by Krishnamurti [17].

In conclusion, we observed and studied the velocity behaviour of non-Boussinesq convective structures — hexagons and asymmetric rolls — in a water layer at 4 °C. As far as we know it is the first time that such a behaviour has been observed in water. The existence of the non-Boussinesq structure as well as the thermal behaviour of the amplitude of convective motion are in agreement with the breakdown of the symmetrical behaviour between ascending and descending velocities due to the non-linear density profile in the water layer.

Acknowledgments. — We wish to thank P. Atten and E. Hopfinger for helpful advice and stimulating discussions.

References

[1] Davis, S. H., *J. Fluid Mech.* **30** (1967), 465.
Davis, S. H., *J. Fluid Mech.* **32** (1968) 619.
Stork, K. and Müller, U., *J. Fluid Mech.* **54** (1972) 599.
[2] Dubois, M. and Bergé, P., *J. Fluid Mech.* **85** (1978) 641.
[3] Farhadieh, R. and Tankin, R. S., *J. Fluid Mech.* **66** (1974) 739.
[4] Oertel, H. and Bühler, K., *Int. J. Mass Heat Transfer* **21** (1978) 1111.
[5] Wesfreid, J., Pomeau, Y., Dubois, M., Normand, C. and Bergé, P., *J. Physique* **39** (1978) 725.
[6] Bénard, H., *Res. Gen. Sci. Pures Appl.* **11** (1900) 1161.
[7] Busse, F. H., *J. Fluid Mech.* **30** (1967) 625.
[8] Palm, E., Ellingsen, T. and Gjévik, B., *J. Fluid Mech.* **30** (1967) 651.
[9] Somerscales, E. and Dougherty, T. S., *J. Fluid Mech.* **42** (1970) 755.
[10] Whitehead, J. A., *Fluctuations, Instabilities and Phase Transitions*, Nato Advanced Study Instituts (Plenum Press) 1975, Vol. **B 11**, p. 153.
[11] Hoard, C., Robertson, C. and Acrivos, A., *Int. J. Heat Mass Transfer* **13** (1970) 849.
[12] Bergé, P., *Fluctuations. Instabilities and Phase Transitions*. Nato Advanced Study Instituts (Plenum Press) 1975, Vol. **B 11** p. 323.
[13] Zu-Shung Sun, Chi-Tien and Yin-Chao Yen, *Aiche J.*, **15** (1969) 910.
[14] Legros, J. C., Longree, D. and Thomaes, G., *Physica* **72** (1974) 410.
[15] Chandrasekhar, S., *Hydrodynamic and Hydromagnetic Stability* (Oxford University Press, London) 1961.
[16] Atten, P. and Lacroix, J. C., Submitted to *J. Méc.* (1978).
[17] Krishnamurti, R., *J. Fluid Mech.* **33** (1968) 445 and 447.
[18] Moore, D. R. and Weiss, N. O., *J. Fluid Mech.* **61** (1973) 553.
[19] Normand, C., Pomeau, Y., Velarde, M. G., *Rev. Mod. Phys.* **49** (1977) 581.
[20] Haken, H., *Rev. Mod. Phys.* **47** (1975) 67.
[21] Veronis, G., *Astrophys. J.* **137** (1963) 641.